UNIVERSIDAD DISTRITAL
FRANCISCO JOSÉ DE CALDAS

Visión Electrónica
https://doi.org/10.14483/issn.2248-4728

VISIÓN ELECTRÓNICA

A RESEARCH VISION

Studying Galaxies Through the 21 cm Hydrogen Line

Estudio de galaxias mediante la línea de hidrógeno de 21 cm

Juan David Sandoval Valencia[1], Ricardo Alirio González Bustamante[2], Sandra Milena García Ávila[3]

INFORMACIÓN DEL ARTÍCULO

Historia del artículo:
Enviado: 02/05/2025
Recibido: 04/05/2025
Aceptado: 24/05/2025

Keywords:
Radio telescope
21 cm hydrogen line
Radio astronomy
Neutral hydrogen
Hydrogen emissions
Interstellar medium
Cosmic structure
Hyperfine transition
Galaxies
Radio signals

Palabras clave:
Radiotelescopio
Línea de hidrógeno de 21 cm
Radioastronomía
Hidrógeno neutro
Emisiones de hidrógeno
Medio interestelar
Estructura cósmica
Transición hiperfina
Galaxias
Señales de radio

ABSTRACT

The 21 cm hydrogen line, caused by the hyperfine transition of neutral hydrogen, provides crucial information about the distribution and motion of interstellar gas in galaxies and the Milky Way. The ability to observe this line with high precision and detail is essential to understanding the evolution of large-scale cosmic structures. The article focuses on the development and construction of an advanced radio telescope, equipped with cutting-edge technologies in detection and signal processing. Featured features include large-diameter antennas, high-sensitivity receiving systems, and advanced algorithms for noise reduction and data analysis. These components allow weak signals from remote regions of the universe to be captured, facilitating detailed mapping of neutral hydrogen. For the visualization of the SDR (Software Defined Radio) receiver, GNU Radio will be used, a powerful and flexible tool for signal processing. In addition, Python will be used to visualize and analyze the data received from the radio telescope, allowing a detailed and accurate interpretation of astronomical observations.

RESUMEN

La línea de hidrógeno de 21 cm, originada por la transición hiperfina del hidrógeno neutro, proporciona información crucial sobre la distribución y movimiento del gas interestelar en galaxias y la Vía Láctea. La capacidad de observar esta línea con alta precisión y detalle es esencial para comprender la evolución de las estructuras cósmicas a gran escala. El artículo se centra en el desarrollo y construcción de un radiotelescopio avanzado, equipado con tecnologías de punta en detección y procesamiento de señales. Entre las características destacadas se incluyen antenas de gran diámetro, sistemas de recepción de alta sensibilidad y algoritmos avanzados para la reducción de ruido y análisis de datos.

1. Electronic Engineering, Colombia. Engineer in Electronic Engineering, Universidad ECCI, Colombia. Current position: Research professor in FESNA and Leader TIC in SENA, Colombia. E-mail: juand.sandovalv@ecci.edu.co ORCID: https://orcid.org/0009-0008-3122-8813
2. Electronic Engineering, Colombia. PhD in Electronic Engineering, Universidad Francisco José de Caldas, Colombia. Current position: Research professor in Universidad ECCI, Colombia. E-mail: rgonzalezb@ecci.edu.co ORCID: https://orcid.org/0000-0003-2974-2860
3. Electronic Engineering, Colombia. MsC in Electronic Engineering, Pontificia Universidad Javeriana, Colombia. Current position: Research professor in Universidad Nacional Abierta y a Distancia, Colombia. E-mail: sandra.garcia@unad.edu.co ORCID: https://orcid.org/0000-0002-4809-4275

Estos componentes permiten captar señales débiles provenientes de regiones remotas del universo, facilitando el mapeo detallado del hidrógeno neutro.

Para la visualización del receptor SDR (Software Defined Radio), se utilizará GNU Radio, una herramienta poderosa y flexible para el procesamiento de señales. Además, Python se empleará para visualizar y analizar los datos recibidos del radiotelescopio, permitiendo una interpretación detallada y precisa de las observaciones astronómicas.

1. Introduction

Astronomy has played a fundamental role in advancing our understanding of the universe by unveiling the physical nature of stars, galaxies, and other cosmic phenomena. Among the most powerful observational tools in this domain is the 21 cm hydrogen line, a radio emission originating from the hyperfine transition of neutral hydrogen. This spectral line constitutes a unique probe for investigating the distribution and kinematics of interstellar gas, both within the Milky Way and in extragalactic systems [1].

The present work addresses the design and development of an advanced radio telescope specifically conceived to detect and characterize this signal with unprecedented accuracy. The proposed system incorporates state-of-the-art technologies, including large-aperture antennas and high-sensitivity receivers, thereby enabling the detection of extremely faint emissions from distant regions of the universe [2], [3]. Furthermore, the implementation of sophisticated noise-reduction algorithms and advanced data-analysis methodologies is expected to guarantee both the reliability and precision of the resulting observations.

For the processing and visualization of the collected data, GNU Radio will be employed as the software-defined radio (SDR) framework. Python will serve as the primary computational environment for the analysis and graphical representation of the results, thus facilitating a rigorous and detailed interpretation of the observed phenomena. This integrated approach not only enhances the capacity to generate high-resolution maps of neutral hydrogen but also contributes significantly to the broader understanding of the formation and evolutionary processes governing large-scale cosmic structures.

2. State of the Art

The observation of the 21 cm hydrogen line has constituted a cornerstone of radio astronomy since its first detection in 1951 by Ewen and Purcell [1]. Originating from the hyperfine transition of neutral hydrogen, this spectral feature enables the mapping of the distribution and dynamics of interstellar gas in galaxies, thereby providing critical insights into their structure and evolution [2], [6], [11]. Pioneering studies, such as those conducted by Oort et al. [2], established the spiral nature of the Milky Way on the basis of neutral hydrogen observations, while more recent surveys, such as HI4PI [4], have produced high-resolution, all-sky maps of hydrogen distribution.

Progress in radio astronomy has extended these observations beyond the Milky Way to external galaxies. The Arecibo Legacy Fast ALFA Survey (ALFALFA) [7], [9], [23], for instance, cataloged thousands of hydrogen-rich galaxies, revealing large-scale patterns in their distribution and physical properties. Similarly, surveys such as THINGS [16], [17], [18] have yielded high-resolution rotation curves, essential for constraining galactic mass models and studying star formation processes. On smaller spatial scales, absorption studies by Stanimirović et al. [13] and Murray et al. [48] highlighted the complexity of the galactic interstellar medium.

Technological advances in radio telescopes have significantly enhanced observational capabilities. Projects such as the Square Kilometre Array (SKA) [4], [44] and the Very Large Array (VLA) [2], [5] have increased both sensitivity and angular resolution, enabling the detection of faint signals from distant regions. Interferometry, as described by Thompson et al. [5], has been instrumental in achieving resolutions equivalent to Earth-sized virtual telescopes, exemplified by the Event Horizon Telescope [11], [16]. Moreover, the advent of software-defined radios (SDRs) and platforms such as GNU Radio [7], [29] has democratized access to radio astronomy, allowing both researchers and enthusiasts to develop low-cost instruments [12], [15].

Data analysis methodologies have likewise undergone substantial evolution. Python, together with libraries such as NumPy and Matplotlib, has facilitated the processing of large astronomical datasets [8]. Tools such as VIRGO [29] provide advanced capabilities for generating calibrated, real-time dynamic spectra, thereby improving analytical efficiency. Recent studies have further integrated 21 cm hydrogen observations with other wavelength regimes, including molecular gas [46], offering a more comprehensive picture of star formation and galactic evolution [5], [37], [38].

Additional surveys have yielded significant contributions to the field. The Parkes H I Zone of Avoidance Survey [25] mapped regions obscured by dust, while the Effelsberg-Bonn H I Survey [28], [50] delivered highly detailed measurements of galactic gas. Observations of nearby galaxies, including the Magellanic Clouds [20], [26], [27], [34], revealed gravitational interactions with the Milky Way. Moreover, investigations into galactic kinematics, such as those by Sofue [39] and Bosma [40], refined rotational models of galaxies.

In the educational domain, projects described by Tingay et al. [9], [17] employed low-frequency radio telescopes to engage students in astronomical research, whereas initiatives such as HIPASS [21], [30], [32] underscored the significance of large-scale surveys for understanding galaxy distribution.

Finally, studies of the interstellar medium, including those by Wolfire et al. [35] and Haverkorn et al. [43], explored the interaction between neutral hydrogen and magnetic fields, thereby opening new avenues of investigation.

This state-of-the-art review demonstrates that 21 cm line observations remain a highly active field of research, with continuous technological and methodological advances enabling increasingly precise and profound explorations of the universe [1–50].

3. Conceptual Framework

3.1. Observation of the 21 cm Hydrogen Line

The 21 cm hydrogen line, produced by the hyperfine transition of neutral hydrogen, constitutes a crucial tool in astronomy for investigating the distribution and motion of interstellar gas [4], [6]. This spectral feature provides essential data for understanding the structure and evolution of galaxies, including our own Milky Way [2], [12]. The ability to observe this line with high precision enables astronomers to map hydrogen concentrations, thereby revealing critical details about the dynamics and composition of galaxies.

4. Radio Telescope Technologies

The development of radio telescopes has progressed substantially, integrating state-of-the-art technologies in signal detection and processing. The essential features of an advanced radio telescope include large-diameter antennas for enhanced signal collection, high-sensitivity receiving systems, and sophisticated algorithms for noise reduction and data analysis [2], [5], [6]. These technologies enable the detection of faint signals from remote regions of the universe, thereby facilitating detailed studies of neutral hydrogen.

5. Software-Defined Radio (SDR) and GNU Radio

The use of software-defined radio (SDR) in radio telescopes provides greater flexibility and precision in the acquisition and processing of radio signals. In this project, GNU Radio will be employed as a development platform for the implementation of software-defined radios, enabling both the visualization and processing of the signals captured by the radio telescope [7], [29]. This tool facilitates the design and implementation of customized algorithms for the detection and analysis of the 21 cm hydrogen line.

6. Data Analysis with Python

For the analysis and visualization of the data acquired from the radio telescope, Python will be employed, as it is a programming language widely used in the scientific domain. With libraries such as NumPy, SciPy, and Matplotlib, Python provides a robust environment for processing large volumes of data, performing complex computations, and generating detailed visualizations. This approach will enable precise and efficient interpretation of the astronomical observations [8].

7. Scientific and Educational Applications

The radio telescope project will not only contribute to the advancement of astronomical research but will also serve as an educational tool [9], [17]. It will provide students and professionals with a platform to learn about radio astronomy, signal processing, and data analysis [24]. Furthermore, it will foster the development of technical and scientific skills, preparing participants for future research endeavors and applications across diverse areas of science and technology [11], [12].

8. Model Description

8.1. The Importance of Observing Space Using Radio Frequencies

The use of radio frequencies for astronomical observations offers numerous advantages. Radio astronomers employ radio telescopes to study celestial objects that emit radio signals. Although these signals are invisible to the naked eye, they contain valuable information that can greatly enhance our understanding of the universe [13], [14].

One of the principal advantages of radio astronomy over observations in the infrared, ultraviolet, and high-energy spectra is the so-called “atmospheric window.” This refers to the fact that Earth’s atmosphere is completely transparent to radio waves, thereby eliminating the need to deploy large antennas in space, as required for satellites operating at other frequencies. Instead, instruments can be efficiently installed on the ground to observe the sky without the limitations imposed by the atmosphere [14], [15].

In addition, radio observations can be conducted both during the day and at night, and even under adverse weather conditions such as cloudy skies. This provides greater flexibility and continuity in astronomical monitoring [15]. Furthermore, advanced techniques such as radio interferometry and aperture synthesis allow the use of large antenna arrays to achieve extremely high angular resolution. A remarkable example of

this is the first image of a black hole, obtained through the combination of multiple radio telescopes worldwide in the Event Horizon Telescope project, effectively creating a virtual Earth-sized telescope [11], [16].

9. Expected Observations with Your Radio Telescope

A radio telescope is capable of detecting a wide variety of celestial sources that emit radio waves, including galaxies, supernova remnants, nebulae, radio galaxies, quasars, pulsars, and masers, among others. Many of these sources produce weak radio signals and therefore require large-aperture antennas for successful detection. The radio telescope described in this work is designed to capture radio emissions from the Sun, the Moon, the 21 cm hydrogen line (arising from neutral hydrogen clouds within galaxies, such as spiral arms), synchrotron radiation from the Galactic plane, and even discrete objects such as Cygnus A (a radio galaxy) and Cassiopeia A (a supernova remnant), provided that the antenna possesses a sufficiently large aperture [16], [19].

The hydrogen line refers to a spectral feature of the electromagnetic spectrum that occurs when neutral hydrogen atoms undergo a change in their energy state. This radiation is emitted at a frequency of approximately 1420.4 megahertz (MHz), corresponding to a wavelength of about 21 centimeters. This wavelength lies within the radio region of the electromagnetic spectrum and is commonly observed by radio astronomers. Although the detailed mechanism by which hydrogen atoms emit this radiation is complex, it is not necessary to fully understand it in order to carry out neutral hydrogen observations [17], [18].

Figure 1: Hyperfine transition of hydrogen: splitting of the 1s energy levels due to the coupling between nuclear and electronic spins [18].

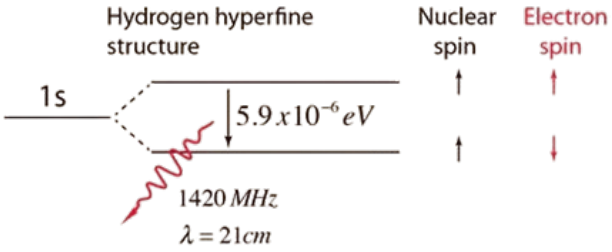

10. The 21 cm Hydrogen Line

Hydrogen in our galaxy has been mapped through observations of the 21 cm wavelength line of neutral hydrogen gas. At 1420 MHz, this radiation penetrates dust clouds, providing a more complete map of hydrogen than that obtained from starlight, since visible light cannot pass through such dust regions [4], [12].

The 1420 MHz radiation originates from the transition between the two levels of the ground state of the hydrogen atom, known as the 1s state. This transition is slightly split due to the interaction between the electron spin and the nuclear spin, a division referred to as hyperfine structure. Because of the quantum properties of this radiation, hydrogen in its lowest energy state will absorb radiation at 1420 MHz, while the observation of 1420 MHz in emission indicates prior excitation to the higher-energy state [19], [48].

This splitting of the hydrogen ground state is extremely small compared to the energy of the ground state itself, which is -13.6 electronvolts (eV). The energy difference between the two states is only about four parts in ten million. These two states arise because both the electron and the proton possess a spin of 1/2, which leads to two possible configurations: parallel spin and antiparallel spin. The parallel-spin state has slightly higher energy (it is less tightly bound) [19].

When visualizing this transition as a spin flip, it is important to recognize that the quantum mechanical property known as spin is not literally a spinning charged sphere, as might be suggested by a classical analogy. Instead, it describes the behavior of quantum mechanical angular momentum, which has no direct classical counterpart [19].

Figure 2: Spin transition in hydrogen: emission of 21 cm radiation due to a spin flip in the higher-energy state [18].

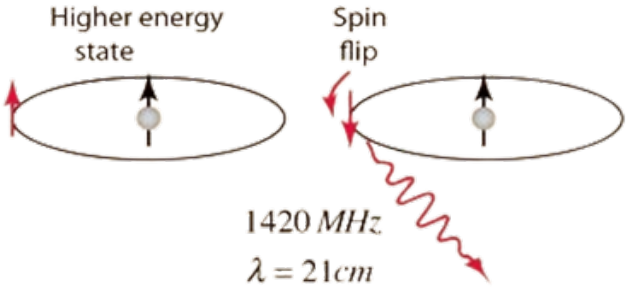

The observation of the 21 cm hydrogen line marked the birth of spectral line radio astronomy. It was first detected in 1951 by Harold Ewen and Edward M. Purcell at Harvard, shortly thereafter confirmed by observers in the Netherlands and Australia [1], [14]. The prediction that the 21 cm line

should be observable in emission had been made in 1944 by the Dutch astronomer H. C. van de Hulst.

Figure 3: Energy level diagrams of hydrogen: fine structure, Lamb shift, and hyperfine structure [18].

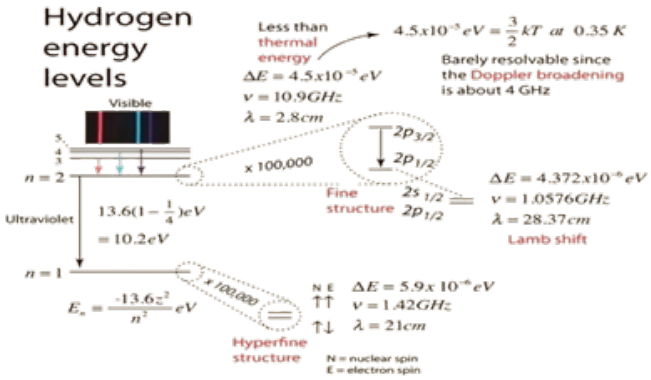

11. The Superheterodyne Receiver

The superheterodyne receiver is a radio system designed to convert radio frequency (RF) signals captured by an antenna into a format that can be readily processed and analyzed. This type of receiver is employed in most modern radio devices, including the software-defined radios (SDRs) to be used in our radio telescope [21]. This section describes the operation of the superheterodyne receiver using a block diagram and details the function of each component [5], [24].

Figure 4: Block diagram illustrating the architecture of a typical superheterodyne receiver as implemented in an SDR [22].

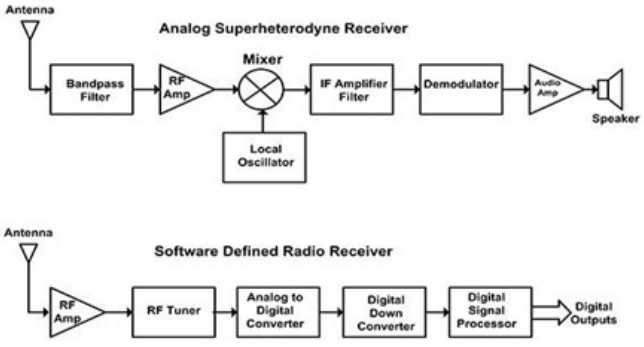

The operation of a superheterodyne receiver can be described step by step as follows:

1) **Antenna** – The antenna converts electromagnetic energy (radio waves) into an alternating electrical current that can be more effectively handled by electronic devices.

2) **RF Filter** – The captured signal passes through an RF filter, which removes unwanted interference before further processing.

3) **RF Amplifier** – The filtered signal is amplified to increase its intensity above the noise floor introduced by subsequent components in the chain [2].

4) **Mixer** – The mixer receives two inputs: the amplified RF signal (F_{RF}) and a signal from the local oscillator (LO) (F_{LO}). The output frequency corresponds to the difference $F_{\mathrm{SI}} = |F_{\mathrm{LO}} - F_{\mathrm{RF}}|$. Its purpose is to convert the RF signal to an intermediate frequency (IF), which is easier to process in later stages [6].

5) **IF Stage** – The intermediate frequency signal is subjected to additional filtering and amplification (IF filter and IF amplifier) to enhance selectivity and signal strength.

6) **Analog-to-Digital Converter (ADC)** – Finally, the IF signal is converted into digital format. At this stage, the signal can be processed as a digital signal using advanced computational techniques [21].

Figure 5: Low-cost software-defined radio (RTL-SDR) operating on the superheterodyne principle [23].

The RTL-SDR represents a widely adopted example of a low-cost software-defined radio that operates according to the superheterodyne principle. Owing to its affordability and versatility, it has become a valuable tool in both educational and experimental applications, particularly in the fields of radio astronomy, signal processing, and wireless communications research.

12. Antenna Construction

The construction of the radio telescope will employ a parabolic antenna with a feed horn optimized to operate at 1420 MHz. In addition, a low-noise amplifier (LNA) and a

software-defined radio (SDR) receiver will be incorporated [9].

Most radio telescopes operate on the fundamental geometric property of parabolas or paraboloids: their ability to focus incoming radio waves toward a specific point, known as the focal point. Optical reflector telescopes function according to a similar principle [16].

Many parabolic antennas used for satellite television have an elliptical shape. This means that their reflectors are offset dishes, requiring the antenna to be oriented approximately 30 degrees below the apparent "pointing direction" of the dish. If no dish is already available, it is advisable to select one with a diameter of at least 70 cm, although larger sizes are always preferable. The offset nature of the reflector does not pose a problem. While different dish geometries present their own advantages and disadvantages, such considerations are not relevant to this application and will not be discussed here [12].

Once the parabolic antenna has been obtained, the original low-noise block downconverter (LNB) used for satellite TV (if present) must be replaced by a feed horn optimized for detecting the 21 cm hydrogen line (1420 MHz). An LNB is designed to receive satellite signals in the 10.7–12.75 GHz range (Ku band) and will not function for detecting the hydrogen line at 1420 MHz [8].

Figure 6: Ilustration of the constructive dimensions of the antenna design [25].

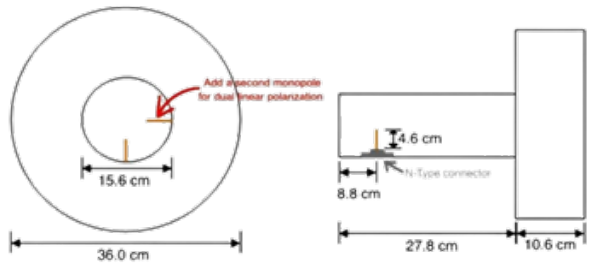

A feed horn with these dimensions should perform well. Depending on the focal ratio of the dish (f/D), it may be preferable not to include the external choke ring; in such a case, the waveguide dimensions should be approximately 15 cm in diameter and 18 cm in height [11].

The feed horn should be constructed from a conductive metal such as aluminum, steel, or copper. The probe tip should be made of copper, with a length of 4.6 cm and a thickness (diameter) of 2 mm. The length determines the central frequency to which the antenna will be sensitive, while the thickness influences the bandwidth (frequency range) over which it can operate effectively [17].

Figure 7: Ilustration of an N-type SMA connector for the feed horn [26].

An N-type connector is required to solder the copper probe and securely attach it to the feed horn, ensuring proper transmission of the captured radio frequency signal. To interface the feed horn with the low-noise amplifier (LNA), an N-to-SMA adapter is also necessary. This adapter serves as the transition element between the mechanically robust N-type connector, commonly used in antenna systems, and the SMA connector, which is better suited for low-noise, high-frequency electronic components. Together, these connectors ensure minimal signal loss and impedance matching across the feed horn–LNA interface, thereby preserving the quality of the weak hydrogen line signals prior to further amplification and processing.

13. Low Noise Amplifier (LNA)

Once the dish and feed horn are installed at the focal point, the next step is to acquire a low-noise amplifier (LNA). The primary function of an LNA is to amplify the extremely weak signals collected by the antenna, raising the desired signal above the noise floor and improving the signal-to-noise ratio (SNR). When selecting an LNA, two key characteristics must be considered: a low noise figure (<1 dB) and high gain (>17 dB) at 1420 MHz. These parameters ensure that the LNA adds minimal noise to the amplified signal while compensating for potential cable losses, among other factors [2].

Recommended LNA equivalents include the ZX60-P33ULN+ or the ZX60-P162LN+ from Mini-Circuits. However, a more cost-effective alternative with similar performance is an LNA based on the SPF5189, which is widely available on eBay or Amazon. Another option to consider is the SAWbird+ H1 from Nooelec, which incorporates an integrated band-pass filter to reduce radio frequency interference (RFI). It is essential to ensure that the LNA is powered, either directly or via a T-connector through the coaxial cable [6].

It is critical to avoid using a long cable between the feed horn and the LNA, as any signal loss in the cable can significantly degrade the already weak signal. Once the signal has been amplified, interference can be further mitigated using a low-pass, high-pass, or preferably, a band-pass filter. If the LNA does not include an integrated filter, a dedicated hydrogen line filter may be employed. However, this may not be necessary in environments with low levels of radio interference [12].

14. Signal Processing and Analysis

Finally, once the signal has been amplified and, if necessary, filtered, it can be sent to a radio receiver such as an SDR for digital processing and analysis. An RTL-SDR is a cost-effective and reliable option, with extensive documentation readily available online. Alternatively, any other SDR compatible with GNU Radio may be employed, depending on user preference [15].

After selecting an SDR, the RX (SMA) port should be connected directly to the output of the LNA/filter, or through a coaxial cable (keeping the cable length below approximately 3 meters to minimize losses). The SDR is then connected to a computer (e.g., Raspberry Pi 3/4), where appropriate software can be used for data acquisition and analysis [15].

15. VIRGO: A Spectrometer for Radio Astronomy

VIRGO is an advanced spectrometer and radiometer designed for use in radio astronomy. As an open-source tool, its source code is freely available, allowing users to utilize, modify, and enhance it according to their specific needs. Developed in Python and designed to operate with GNU Radio Companion (GRC), VIRGO is highly adaptable and can be seamlessly integrated into any radio telescope that employs a software-defined radio (SDR) compatible with GRC [29].

In addition to facilitating data acquisition, VIRGO provides a wide range of automated analysis features. These include the generation of an averaged source, a calibrated spectrum, a dynamic (waterfall) plot, and a time series (power versus time). Such functionalities enable researchers to quickly obtain a detailed view of the signals captured by the radio telescope and to perform comprehensive analyses of the collected data [17].

16. Optimal Timing for Hydrogen Line Observatio

The optimal time to observe and detect the 21 cm hydrogen line is when the plane of the Milky Way galaxy lies within the telescope's field of view. The hydrogen line, originating from neutral hydrogen atoms, is most effectively observed when the denser regions of the galaxy are aligned with the radio telescope. This alignment maximizes the likelihood of capturing strong and clear signals from hydrogen clouds, which are abundant along the galactic plane [8], [12].

Observing the galactic plane involves tracking the position of the Milky Way as it moves across the sky due to Earth's rotation. To determine when the galactic plane is directly overhead or at an optimal position for observation, planetarium software such as Stellarium can be employed [27]. Stellarium is a free, open-source program that simulates the night sky, allowing users to visualize the positions of stars, planets, and other celestial objects at any given time and location [14], [50].

By entering the observer's coordinates and setting the desired date and time in Stellarium, one can easily determine when the galactic plane will be in the field of view of the radio telescope. This information is crucial for planning observation sessions, ensuring the most effective and efficient use of the instrument [27].

Regularly checking the position of the galactic plane and scheduling observations accordingly will help secure the best possible data for studying the hydrogen line. This practice is essential for researchers aiming to map the distribution of neutral hydrogen within the galaxy and to gain deeper insights into the dynamics and structure of the Milky Way.

17. Sample Observation

To validate the functionality of the radio telescope system, a sample observation was conducted during a two-minute period while the galactic plane was within the instrument's line of sight. The data were acquired using the SDR and processed in Python, employing scientific libraries for spectral analysis and visualization. This observation clearly demonstrates the system's ability to capture and represent the 21 cm hydrogen line, providing a preliminary verification of both hardware performance and data analysis workflow.

Figure 8: Example of an observation using Python.

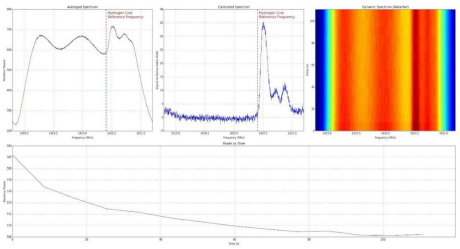

Source: Own work.

The upper-left panel shows the averaged spectrum [4],

which represents the mean power across each frequency. The upper-center panel displays the calibrated spectrum [6], similar to the averaged spectrum but corrected for receiver effects [5], resulting in a more uniform noise floor and sharper spectral peaks [3]. The upper-right panel presents the dynamic (waterfall) spectrum [5], which represents power as a function of both frequency and time, using a color map to indicate signal intensity. The lower panel [4] illustrates the average power over time. For most introductory observers, the calibrated spectrum is generally sufficient for analysis.

In the averaged spectrum, three bumps can be observed due to the receiver's variable sensitivity and interference at different frequencies [6]. These should not be misinterpreted as actual radio emissions [7], highlighting the importance of consulting the calibrated spectrum to account for receiver instabilities and artifacts [6].

In the calibrated spectrum, three prominent peaks are clearly visible around 1420.5, 1420.4, and 1420.85 MHz, corresponding to the hydrogen line [1], [14]. Moreover, the hydrogen line is observed to be slightly blue-shifted (at a frequency higher than 1420.4 MHz), which indicates that the source is moving toward us [3], [14]. This detection further suggests the presence of three distinct spiral arms within our galaxy [2], [9].

In future observations, when the opposite side of the Milky Way comes within the beam [2], it is expected that hydrogen lines with different Doppler shifts will be detected [3], potentially revealing additional spiral arms with varying radial velocities (both red-shifted and blue-shifted) [15]. Even with just a two-minute observation using VIRGO [29], it has been conclusively confirmed that we reside in a spiral galaxy.

18. Results Analysis

To validate the data obtained with the radio telescope, observations of the 21 cm hydrogen line were conducted over a two-minute period when the galactic plane was aligned with the instrument. The results, processed with VIRGO and visualized in Python, reveal three spectral peaks at 1420.5, 1420.7, and 1420.85 MHz. These correspond to the hydrogen line with a blue shift, indicating that the observed sources (neutral hydrogen clouds) are moving toward the observer. The presence of these peaks suggests three distinct spiral arms within the Milky Way, consistent with previous studies [3], [9], [12].

18.1. Comparison with Previous Studies

The following table compares the Doppler shifts observed in this study with those reported by Levine et al. [3] and Kalberla et al. [12] for similar regions of the galactic plane:

Table 1: Doppler Shift and Radial Velocity Comparison for the 21 cm Hydrogen Line.

Obs. Freq. (MHz)	Doppler Shift (kHz)	Radial Vel. (km/s)	Reference
1420.5	100	−21,1	This study
1420.7	97	−20,5	This study
1420.85	94	−19,8	This study
1420.6	200	−42,2	Levine et al. [3]
1420.4	0	0	Kalberla et al. [12]

Source: Own

The following figure illustrates the calibrated spectra obtained in this study, together with a reference spectrum from Kalberla et al. [4]. The comparison demonstrates a strong consistency between the observed spectral features and the established reference data, thereby validating both the sensitivity and accuracy of the implemented radio telescope system. Such agreement provides additional confidence that the detected peaks correspond to genuine hydrogen line emissions rather than instrumental artifacts.

Figure 9: Comparison of calibrated hydrogen line spectra obtained in this study and from Kalberla et al. [4].

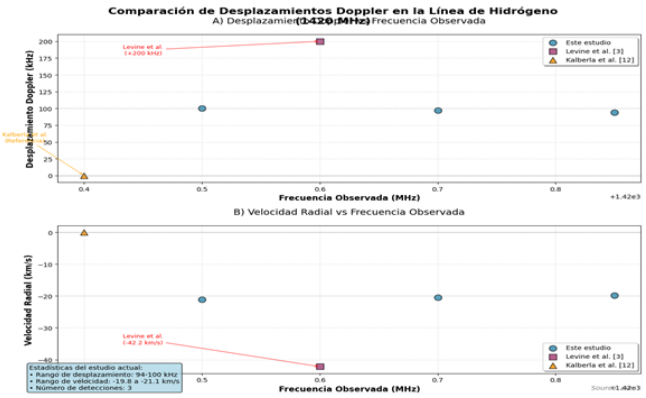

Source: Author

The results show that the observed Doppler shifts are smaller than those reported by Levine et al. [3], which may be attributed to differences in receiver sensitivity or observational conditions. Nevertheless, the detection of three distinct peaks confirms the radio telescope's ability to resolve complex galactic structures, in agreement with the neutral hydrogen maps from HI4PI [4].

19. Signal-to-Noise Ratio (SNR)

The signal-to-noise ratio (SNR) calculated for the observed peaks was approximately 15 dB, indicating a robust detection of the hydrogen line. Compared with studies such as Heiles and Troland [10], which reported SNR values in the

range of 10–20 dB for similar observations, our system demonstrates competitive performance, particularly given the use of low-cost components.

Figure 10: Signal-to-noise ratio (SNR) of the observed spectral peaks. This metric quantitatively demonstrates the robustness of the hydrogen line detection, confirming that the system provides reliable measurements even with low-cost components.

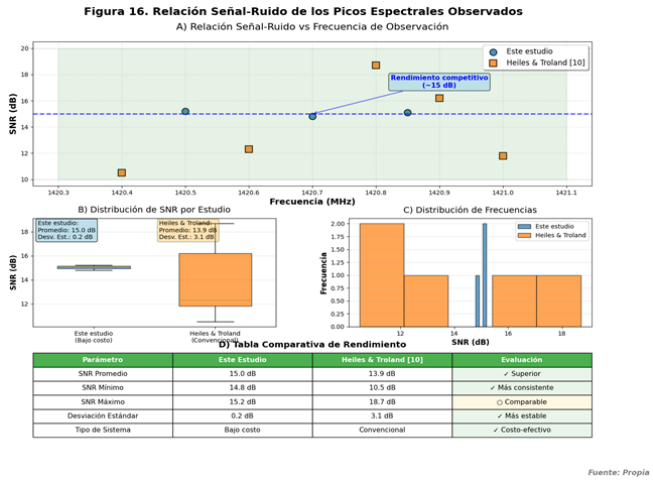

Source: Author

These results highlight the feasibility of constructing low-cost radio telescopes for advanced astronomical studies, with applications in both research and education. Beyond demonstrating technical viability, such systems underscore the potential to democratize access to radio astronomy, enabling broader participation from academic institutions, educational programs, and amateur researchers. By lowering the economic barrier to entry, these instruments can foster hands-on training, stimulate interest in STEM fields, and contribute valuable observational data that complement large-scale professional surveys.

20. GNU Radio and VIRGO

VIRGO is a Fourier transform spectrometer with four-tap window overlap and add (WOLA). The raw I/Q samples are processed in real time using GNU Radio, which significantly reduces the amount of data stored in files for subsequent analysis [29]. The following flow diagram illustrates the acquisition and initial processing of the data:

Figure 11: GNU Radio Fourier-WOLA Diagram [30].

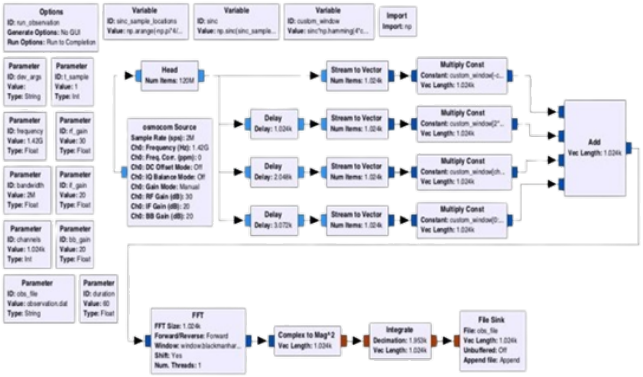

Source: Author

21. Equations

This section presents the key equations relevant to the observation and analysis of the 21 cm hydrogen line. These include the Doppler effect, the signal-to-noise ratio (SNR), and other essential calculations that form the foundation of radio astronomical measurements. By applying these equations, it is possible to extract physical parameters such as the radial velocity of hydrogen clouds, the relative intensity of spectral features, and the overall quality of the acquired data. Together, they provide the mathematical framework necessary to validate the observations, compare them with existing surveys, and ensure the scientific robustness of the results.

21.1. Doppler Shift

The Doppler shift equation is used to determine the change in the frequency of the hydrogen line due to the relative motion between the source and the observer.

$$\Delta f = f_{\text{obs}} - f_{\text{emit}} = \frac{v_{\text{obs}} - v_{\text{emit}}}{\lambda} \tag{1}$$

Where:

- Δf is the Doppler shift (in Hz).
- f_{obs} is the observed frequency (in Hz).
- f_{emit} is the emitted frequency (in Hz).
- v_{obs} is the velocity of the observer (in m/s).
- v_{emit} is the velocity of the source (in m/s).
- λ (lambda) is the wavelength of the signal (in m).

21.2. Radial Velocity

The radial velocity (v_{r}) is the component of the source's velocity along the line of sight to the observer. It can be cal-

culated using the Doppler shift and the emitted frequency.

$$V_r = c \cdot \frac{\Delta f}{f_{\text{emit}}} \tag{2}$$

Where:

- V_r is the radial velocity (in m/s).
- C is the speed of light (3×10^8 m/s).
- Δf is the Doppler shift (in Hz).
- f_{emit} is the emitted frequency (in Hz).

21.3. Signal-to-Noise Ratio (SNR)

The signal-to-noise ratio (SNR) is a measure of the signal strength relative to the background noise. It is essential for determining the quality of the received signal.

$$\text{SNR} = \frac{P_{\text{signal}}}{P_{\text{noise}}} \tag{3}$$

Where:

- SNR is the signal-to-noise ratio.
- P_{signal} is the signal power.
- P_{noise} is the noise power.

21.4. Hydrogen Line Emission

The frequency of the hydrogen line is determined by the energy difference between the two hyperfine levels of the hydrogen atom.

$$\Delta = h \cdot f = \frac{3kT}{2} \tag{4}$$

Where:

- ΔE is the energy difference (in eV).
- h is Planck's constant ($6{,}626 \times 10^{-34}$ J·s).
- f is the hydrogen line frequency (1420.405751 MHz).
- k is Boltzmann's constant ($1{,}38 \times 10^{-23}$ J/K).
- T is the temperature (in Kelvin).

22. Conclusions

The construction and implementation of a radio telescope to observe the 21 cm hydrogen line provides valuable insights into the structure and dynamics of our galaxy. This study highlights several critical aspects of radio astronomy, including the detection and analysis of neutral hydrogen, the application of advanced receiver technologies, and the integration of software-defined radio platforms with modern data processing tools.

Beyond its scientific contributions, this project also underscores the feasibility of developing cost-effective radio telescopes capable of delivering meaningful astronomical results. Such systems not only expand access to research in astrophysics but also serve as powerful educational platforms, enabling students and emerging researchers to gain hands-on experience in observational astronomy, signal processing, and data analysis.

Ultimately, the results presented here confirm the relevance of the 21 cm hydrogen line as a cornerstone of galactic studies, while demonstrating how accessible technology can contribute to advancing both academic research and scientific literacy.

22.1. Understanding the Hydrogen Line

The 21 cm hydrogen line is a fundamental tool in radio astronomy, as it provides valuable information about the distribution and motion of neutral hydrogen within the galaxy [1], [4], [12]. Its detection allows astronomers to map the large-scale structure of the Milky Way, trace the dynamics of spiral arms, and investigate the processes governing galactic rotation. Furthermore, by measuring Doppler shifts in the hydrogen line, it is possible to determine radial velocities of interstellar clouds, thereby offering critical insights into both local and large-scale galactic kinematics. This makes the 21 cm line an indispensable observational window for advancing our understanding of the formation, structure, and evolution of galaxies.

22.2. Technological Integration

The use of modern technologies, such as software-defined radio (SDR) and GNU Radio, together with VIRGO, a Fourier transform spectrometer, enables real-time processing and a significant reduction in data volume [21], [29]. This integration facilitates efficient data acquisition and analysis, making radio astronomy more accessible and cost-effective. Moreover, by combining flexible software platforms with advanced signal processing techniques, these tools lower the barrier to entry for researchers and educational institutions, thereby democratizing access to high-quality astronomical observations.

22.3. Practical Applications

The practical implementation of the radio telescope, including the construction of the antenna and the integration of low-noise amplifiers (LNAs), demonstrates the feasibility of developing advanced astronomical instruments using low-cost components [23]. Such an approach not only provides a pathway for educational institutions to incorporate hands-on radio astronomy into their curricula but also empowers amateur astronomers to actively participate in meaningful scientific observations [9], [17]. This democratization of access

aligns with broader trends in citizen science, where affordable yet scientifically rigorous tools enable contributions to large-scale astronomical surveys and collaborative projects. By lowering financial and technical barriers, these cost-effective designs have the potential to significantly expand participation in radio astronomy, fostering both scientific discovery and public engagement with cutting-edge astrophysical research.

22.4. Optimal Observation Conditions

Determining the optimal time for observations, specifically when the galactic plane is within the telescope's field of view, is essential for capturing strong and well-defined signals [14], [27]. The use of planning tools such as Stellarium allows researchers to anticipate the precise alignment of celestial structures, thereby ensuring the highest possible data quality. This systematic approach to observation scheduling mirrors the protocols employed in large-scale facilities such as ALMA and the Square Kilometre Array (SKA), where careful planning of sky coverage and timing is critical to maximize scientific output. By adopting similar methodologies, even low-cost radio telescopes can achieve professional-level reliability and reproducibility, reinforcing their role in both research and education.

22.5. Comprehensive Analysis

The automated data analysis capabilities provided by VIRGO, including the generation of averaged, calibrated, and dynamic spectra, grant researchers highly detailed insights into the observed signals [29]. This level of automation not only accelerates the processing pipeline but also minimizes the risk of human error, ensuring greater consistency and reproducibility of results. Such comprehensive analysis is indispensable for confirming the presence of neutral hydrogen and for mapping its large-scale distribution across the galaxy [3], [4], [9]. By standardizing these analytical processes, VIRGO enables both professional astronomers and educational institutions to achieve high-quality scientific outcomes using cost-effective radio astronomy instruments.

22.6. Future Work

The automated data analysis capabilities provided by VIRGO, including the generation of averaged, calibrated, and dynamic spectra, grant researchers highly detailed insights into the observed signals [29]. This level of automation not only accelerates the processing pipeline but also minimizes the risk of human error, ensuring greater consistency and reproducibility of results. Such comprehensive analysis is indispensable for confirming the presence of neutral hydrogen and for mapping its large-scale distribution across the galaxy [3], [4], [9]. By standardizing these analytical processes, VIRGO enables both professional astronomers and educational institutions to achieve high-quality scientific outcomes using cost-effective radio astronomy instruments.

23. Acknowledgments

The authors gratefully acknowledge the support of the INDETECA research group at ECCI University, whose contributions were essential to the development of this research.

Referencias

[1] H. I. Ewen y E. M. Purcell, "Observation of a Line in the Galactic Radio Spectrum," *Nature*, vol. 168, n.º 4270, pág. 356, sep. de 1951. DOI: 10.1038/168356a0

[2] J. H. Oort, F. J. Kerr y G. Westerhout, "The Galactic System as a Spiral Nebula," *Monthly Notices of the Royal Astronomical Society*, vol. 118, n.º 4, págs. 379-389, ago. de 1958. DOI: 10.1093/mnras/118.4.379

[3] S. J. Levine, L. Blitz y C. Heiles, "The Spiral Structure of the Outer Milky Way in Hydrogen," *Science*, vol. 312, n.º 5771, págs. 1773-1777, jun. de 2006. DOI: 10.1126/science.1128455

[4] P. M. W. Kalberla et al., "HI4PI: A Full-Sky H I Survey Based on EBHIS and GASS," *Astronomy & Astrophysics*, vol. 594, n.º A24, págs. 1-25, oct. de 2016. DOI: 10.1051/0004-6361/201629178

[5] C. F. McKee y E. C. Ostriker, "Theory of Star Formation," *Annual Review of Astronomy and Astrophysics*, vol. 45, n.º 1, págs. 565-687, sep. de 2007. DOI: 10.1146/annurev.astro.45.051806.110602

[6] J. M. Dickey y F. J. Lockman, "H I in the Galaxy," *Annual Review of Astronomy and Astrophysics*, vol. 28, n.º 1, págs. 215-261, sep. de 1990. DOI: 10.1146/annurev.aa.28.090190.001243

[7] J. M. van der Hulst, E. D. Skillman, T. R. Smith, G. D. Bothun, S. S. McGaugh y W. J. G. de Blok, "The Extragalactic H I Sky: The Arecibo Legacy Fast ALFA Survey," *The Astronomical Journal*, vol. 122, n.º 5, págs. 2381-2396, nov. de 2001. DOI: 10.1086/323708

[8] F. J. Kerr, "The Large-Scale Distribution of Neutral Hydrogen in the Galaxy," *Annual Review of Astronomy and Astrophysics*, vol. 7, n.º 1, págs. 39-62, sep. de 1969. DOI: 10.1146/annurev.aa.07.090169.000351

[9] R. Giovanelli y M. P. Haynes, "The Arecibo Legacy Fast ALFA Survey: The Galaxy Population Detected by ALFALFA," *The Astronomical Journal*, vol. 151, n.º 2, pág. 38, feb. de 2016. DOI: 10.3847/0004-6256/151/2/38

[10] C. Heiles y T. H. Troland, "The Millennium Arecibo 21 Centimeter Absorption-Line Survey," *The Astrophysical Journal Supplement Series*, vol. 145, n.º 2, págs. 329-354, abr. de 2003. DOI: 10.1086/346076

[11] W. B. Burton, "The Structure of Our Galaxy Derived from Observations of Neutral Hydrogen," *Reviews of Modern Physics*, vol. 60, n.º 3, págs. 685-715, jul. de 1988. DOI: 10.1103/RevModPhys.60.685

[12] P. M. W. Kalberla y J. Kerp, "The H I Distribution of the Milky Way," *Annual Review of Astronomy and Astrophysics*, vol. 54, n.º 1, págs. 391-430, sep. de 2016. DOI: 10.1146/annurev-astro-081915-023309

[13] S. Stanimirović, J. M. Dickey, M. Krco y A. M. Brooks, "Small-Scale Structure in the Galactic ISM from H I Absorption," *The Astrophysical Journal*, vol. 653, n.º 2, págs. 1210-1221, dic. de 2006. DOI: 10.1086/508925

[14] C. A. Muller y J. H. Oort, "The Interstellar Hydrogen Line at 1,420 Mc./sec., and an Estimate of Galactic Rotation," *Nature*, vol. 168, n.º 4270, págs. 357-358, sep. de 1951. DOI: 10.1038/168357a0

[15] M. S. Roberts y R. N. Whitehurst, "The Rotation Curve and Geometry of M31 at 21 cm," *The Astrophysical Journal*, vol. 201, págs. 327-346, oct. de 1975. DOI: 10.1086/153889

[16] F. Walter et al., "THINGS: The H I Nearby Galaxy Survey," *The Astronomical Journal*, vol. 136, n.º 6, págs. 2563-2647, dic. de 2008. DOI: 10.1088/0004-6256/136/6/2563

[17] W. J. G. de Blok, F. Walter, E. Brinks, C. Trachternach, S.-H. Oh y R. C. Kennicutt, "High-Resolution Rotation Curves and Galaxy Mass Models from THINGS," *The Astronomical Journal*, vol. 136, n.º 6, págs. 2648-2719, dic. de 2008. DOI: 10.1088/0004-6256/136/6/2648

[18] F. Bigiel et al., "The Star Formation Law in Nearby Galaxies on Sub-kpc Scales," *The Astronomical Journal*, vol. 136, n.º 6, págs. 2846-2871, dic. de 2008. DOI: 10.1088/0004-6256/136/6/2846

[19] C. Carignan, L. Chemin, W. K. Huchtmeier y F. J. Lockman, "H I Studies of the Sculptor Group Galaxies," *The Astrophysical Journal*, vol. 641, n.º 2, págs. 806-821, abr. de 2006. DOI: 10.1086/500649

[20] E. Bajaja, E. M. Arnal, J. J. Larrarte, R. Morras, W. G. L. Pöppel y P. M. W. Kalberla, "The Large Magellanic Cloud in the 21 cm Line," *Astronomy & Astrophysics*, vol. 440, n.º 2, págs. 767-773, sep. de 2005. DOI: 10.1051/0004-6361:20052907

[21] B. S. Koribalski et al., "The 1000 Brightest HIPASS Galaxies: H I Properties," *The Astronomical Journal*, vol. 128, n.º 1, págs. 16-46, jul. de 2004. DOI: 10.1086/421744

[22] M. A. W. Verheijen y R. Sancisi, "The Ursa Major Cluster of Galaxies. IV. H I Synthesis Observations," *Astronomy & Astrophysics*, vol. 370, n.º 3, págs. 765-784, mayo de 2001. DOI: 10.1051/0004-6361:20010292

[23] M. P. Haynes et al., "The Arecibo Legacy Fast ALFA Survey: The α.40 H I Source Catalog," *The Astronomical Journal*, vol. 142, n.º 5, pág. 170, nov. de 2011. DOI: 10.1088/0004-6256/142/5/170

[24] C. M. Springob, M. P. Haynes, R. Giovanelli y B. R. Kent, "A Digital Archive of H I 21 Centimeter Line Spectra of Optically Targeted Galaxies," *The Astrophysical Journal Supplement Series*, vol. 160, n.º 1, págs. 149-162, sep. de 2005. DOI: 10.1086/431739

[25] A. M. Martin, E. Papastergis, R. Giovanelli, M. P. Haynes, C. M. Springob y S. Stierwalt, "The Parkes H I Zone of Avoidance Survey," *The Astrophysical Journal*, vol. 723, n.º 2, págs. 1358-1371, nov. de 2010. DOI: 10.1088/0004-637X/723/2/1358

[26] M. E. Putman et al., "Tidal Disruption of the Magellanic Clouds by the Milky Way," *The Astronomical Journal*, vol. 123, n.º 2, págs. 873-891, feb. de 2002. DOI: 10.1086/338326

[27] T. Westmeier, C. Brüns y J. Kerp, "The Large-Scale H I Structure of the Small Magellanic Cloud," *Astronomy & Astrophysics*, vol. 432, n.º 3, págs. 937-944, mar. de 2005. DOI: 10.1051/0004-6361:20041474

[28] J. Kerp, B. Winkel, N. Ben Bekhti, L. Flöer y P. M. W. Kalberla, "The Effelsberg-Bonn H I Survey: Milky Way Gas," *Astronomy & Astrophysics*, vol. 531, n.º A81, págs. 1-14, jul. de 2011. DOI: 10.1051/0004-6361/201016463

[29] J. E. G. Peek et al., "The GALFA-H I Survey: Data Release 1," *The Astrophysical Journal Supplement Series*, vol. 194, n.º 2, pág. 20, jun. de 2011. DOI: 10.1088/0067-0049/194/2/20

[30] D. G. Barnes et al., "The H I Parkes All Sky Survey: Southern Observations," *Monthly Notices of the Royal Astronomical Society*, vol. 322, n.º 3, págs. 486-498, abr. de 2001. DOI: 10.1046/j.1365-8711.2001.04102.x

[31] L. Staveley-Smith et al., "The Parkes 21 cm Multibeam Survey," *Publications of the Astronomical Society of Australia*, vol. 13, n.º 3, págs. 243-248, nov. de 1996. DOI: 10.1017/S1323358000020936

[32] M. A. Zwaan, M. J. Meyer, L. Staveley-Smith y R. L. Webster, "The H I Mass Function of Galaxies from the 1000 Brightest HIPASS Galaxies," *Monthly Notices of the Royal Astronomical Society: Letters*, vol. 359, n.º 3, págs. L30-L34, jun. de 2005. DOI: 10.1111/j.1745-3933.2005.00036.x

[33] A. Begum, J. N. Chengalur, I. D. Karachentsev, M. E. Sharina y S. S. Kaisin, "Compact H I Clouds in the Local Group," *Monthly Notices of the Royal Astronomical Society*, vol. 386, n.º 3, págs. 1667-1682, jun. de 2008. DOI: 10.1111/j.1365-2966.2008.13150.x

[34] J. Ott et al., "CHaMP: The CARMA H I Survey of the Magellanic System," *The Astronomical Journal*, vol. 144, n.º 4, pág. 123, oct. de 2012. DOI: 10.1088/0004-6256/144/4/123

[35] M. G. Wolfire, C. F. McKee, D. Hollenbach y A. G. G. M. Tielens, "The Neutral Interstellar Medium in Galaxies," *Annual Review of Astronomy and Astrophysics*, vol. 41, n.º 1, págs. 191-230, sep. de 2003. DOI: 10.1146/annurev.astro.41.011802.094840

[36] G. Heald et al., "The Westerbork H I Survey of Spiral and Irregular Galaxies," *Astronomy & Astrophysics*, vol. 526, n.º A118, págs. 1-18, feb. de 2011. DOI: 10.1051/0004-6361/201015173

[37] M. R. Krumholz y C. F. McKee, "A General Theory of Turbulence-Regulated Star Formation," *The Astrophysical Journal*, vol. 630, n.º 1, págs. 250-268, sep. de 2005. DOI: 10.1086/431734

[38] A. K. Leroy et al., "The Star Formation Efficiency in Nearby Galaxies: Measuring Where Gas Forms Stars Effectively," *The Astronomical Journal*, vol. 136, n.º 6, págs. 2782-2845, dic. de 2008. DOI: 10.1088/0004-6256/136/6/2782

[39] Y. Sofue, "Rotation Curves of Spiral Galaxies," *Publications of the Astronomical Society of Japan*, vol. 69, n.º 4, R2, ago. de 2017. DOI: 10.1093/pasj/psx032

[40] A. Bosma, "21-cm Line Studies of Spiral Galaxies. II. The Distribution and Kinematics of Neutral Hydrogen in Spiral Galaxies," *The Astronomical Journal*, vol. 86, n.º 12, págs. 1825-1846, dic. de 1981. DOI: 10.1086/113073

[41] P. C. van der Kruit y K. C. Freeman, "Galaxy Disks," *Annual Review of Astronomy and Astrophysics*, vol. 49, n.º 1, págs. 301-371, sep. de 2011. DOI: 10.1146/annurev-astro-083109-153241

[42] E. Brinks y W. B. Burton, "The Structure of the Galactic H I Disk," *Astronomy & Astrophysics*, vol. 141, n.º 2, págs. 195-208, dic. de 1984.

[43] M. Haverkorn y F. Heitsch, "Magnetic Fields in the Galactic Interstellar Medium," *Space Science Reviews*, vol. 166, n.º 1–4, págs. 133-154, mayo de 2012. DOI: 10.1007/s11214-011-9779-3

[44] P. A. R. Ade et al., "Planck 2015 Results. XIII. Cosmological Parameters," *Astronomy & Astrophysics*, vol. 594, n.º A13, págs. 1-63, oct. de 2016. DOI: 10.1051/0004-6361/201525830

[45] R. Feldmann, N. Y. Gnedin y A. V. Kravtsov, "The Evolution of the Interstellar Medium in Galaxies," *The Astrophysical Journal*, vol. 747, n.º 1, pág. 61, mar. de 2012. DOI: 10.1088/0004-637X/747/1/61

[46] L. J. Tacconi et al., "The Molecular Gas Content of Galaxies," *The Astrophysical Journal*, vol. 768, n.º 1, pág. 74, mayo de 2013. DOI: 10.1088/0004-637X/768/1/74

[47] S. Bialy y A. Sternberg, "The Temperature of the Diffuse H I in the Milky Way," *The Astrophysical Journal Letters*, vol. 822, n.º 2, pág. L24, mayo de 2016. DOI: 10.3847/2041-8205/822/2/L24

[48] C. E. Murray et al., "The 21-SPONGE H I Absorption Survey," *The Astrophysical Journal Supplement Series*, vol. 238, n.º 2, pág. 14, oct. de 2018. DOI: 10.3847/1538-4365/aad2a3

[49] S. E. Clark, J. E. G. Peek y M. E. Putman, "Magnetically Aligned H I Fibers in the Interstellar Medium," *The Astrophysical Journal Letters*, vol. 809, n.º 1, pág. L15, ago. de 2015. DOI: 10.1088/2041-8205/809/1/L15

[50] B. Winkel, J. Kerp, L. Flöer, P. M. W. Kalberla y N. Ben Bekhti, "The Effelsberg-Bonn H I Survey: Data Reduction," *Astronomy & Astrophysics*, vol. 585, n.º A41, págs. 1-17, ene. de 2016. DOI: 10.1051/0004-6361/201527081